Features of Log-periodic Acceleration in Fluctuations of Sun Irradiation.

Sergey Feranchuk, Smolensk State University, feranchuk@gmail.com

Abstract

Background. Level of Sun irradiation continously changes at any scale of time; some features of self-affinity are anyway expected there. "Ideal" self-affinity imply a presence of a linear dependence between a scale of fluctuations and a scale of time; a slope of that line is a value of "fractal dimension". The "scale-vs.-scale" distributions for the fluctuations of Sun irradiation are not linear, a slope of the fitting line depends on time and a diapason of scales.

Chaotic processes like the burning of Sun are anyway characterized, also, by a presence of some slow-scale oscillations and sudden outbreaks. A property of log-periodicity is another side of "fractal"-like distributions, it can be applied to describe these oscillations, and it imply either inceasing or decreasing of their periodicity. Increased periodicity of chaotic outbreaks can warn about the approaching "crash", a "phase transition", a loss of any stability in an observed "world".

Methods. A presence of log-periodic oscillations would influence a scale of time, and relative positions of sequential measurements along the axis of time. A scale distributions of Sun irradiation were compared for a couple of data sources, a presence of log-periodicity was approached trying to guess a best fit of the linear dependency for data points with modified time-axis positions. The approach was comparatively applied to fluctuations of water temperature in Baikal, were a crisis happened in around 2014.

Results. In early period before the crisis in Baikal, between 2010 and 2012, the scale diastribution for water temperature within a range from hours to several days looks different than in later another periods, and the attempts to apply the law of log-periodicity to this distribution appear to be ... . The same ... for the fluctuations of MgII Sun irradiation between 1978 and 2004.

Conclusion

Introduction

The burning of Sun attracts attention of many physicists, and modern techniques of measurements are able to supply experimental data of various types. From the variety of approaches, two time series of measurements are shown in figure 1. Long-time observations are able to detect a presence of "solar cycles", regular changes of the burning intensity, 14-years cycle contributed the most to the variations of the intensity, as it can be seen in fig 1A. In the periods of instability, the burning of Sun is more ...
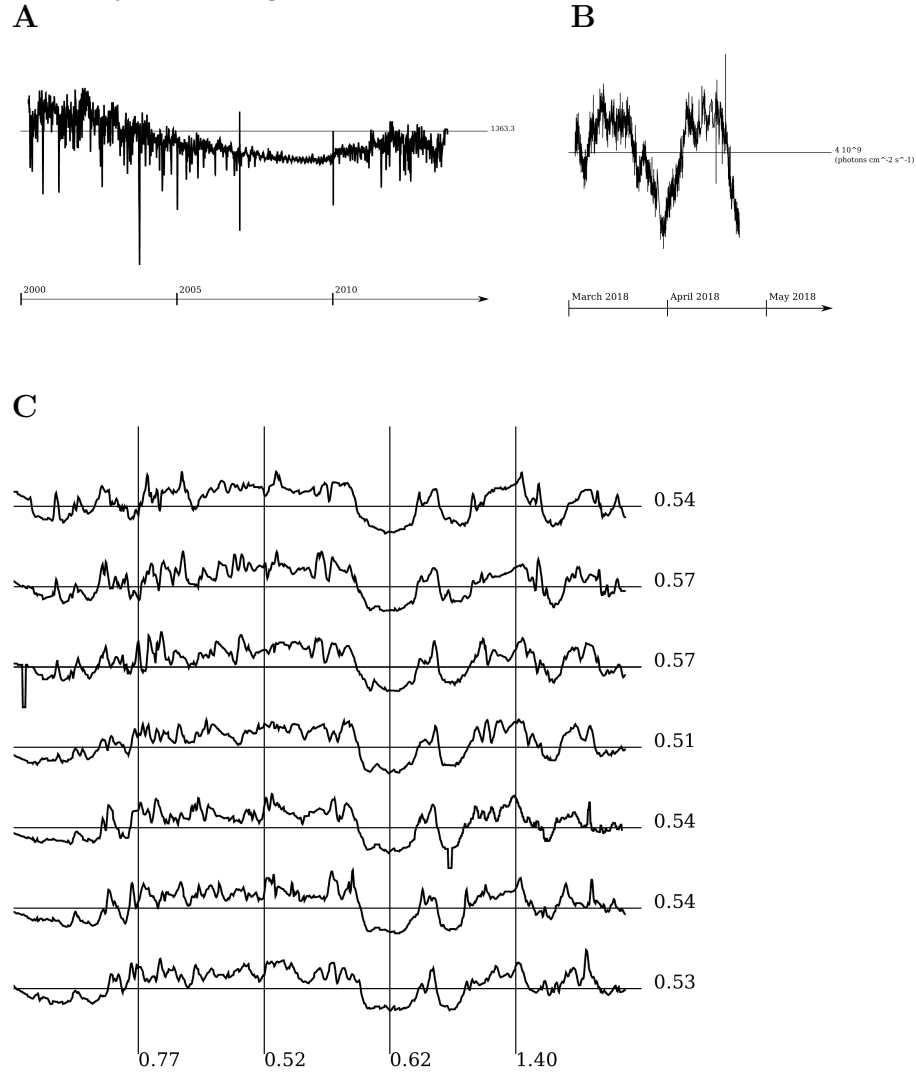
A

B

1363.3

$4 \cdot 10^9$
(photons cm^-2 s^-1)

2000   2005   2010

March 2018   April 2018   May 2018

C

0.54

0.57

0.57

0.51

0.54

0.54

0.53

0.77   0.52   0.62   1.40

Figure 1 *(A) Radiation of Sun from 2000 to 2013 recorded by "ACRIM3" satellite; (B) Extracts form satellite data records of photon flux deposited in Univ. of South Carolina site, radiation of Sun in 2018; (C) Snapshot from video record of sun flaming 15.06.2002, deposited by Swedish physicists.*
in C, digits in column - Higuchi fractal dimension for spatial axis, digits in row -

approximation of fractal dimension for time axis.

The two approches are ... to measure the scale of fluctuations depending on a scale of time; first is known as "Higuchi" dimension [1], second was proposed by Peng et al [2] ...

The generic linkage between "fractal" properties and a presence of log-periodicity was observed and described ... in part in theory, in part in some applied cases... [3].

"Naive" ways to observe some log-periodicity ... can point at most to an expected periodic "burst" ... some is demonstrated above in fig 1C.

Methods

Fitting of log-periodicity

Log-periodic perturbation f depends on a time t by a definition as written below:

$t < t_c, f \sim \sin(\omega \log(t_c - t))$

$t > t_c, f \sim \sin(\omega \log(t - t_c))$

There, a critical time t_c and a frequency of transformed oscillations ω are a minimal set of parameters for any log-periodicity. Peaks of this distribution which can be ... to outbreaks in an observed "world" are located at positions defined by expression $2\pi i = \omega \log(t_c - t_i), i = 1, 2, ..., n, ...$ (for a case $t < t_c$).

Let the observed distribution is in bounds between n_m and n_M of the assumend log-periodicity, that is, $\omega \log(t_{max} - t_c) = n_m, \omega \log(t_{min} - t_c) = n_M$, or *vice versa*. The period ω would be then $\omega = \log(n_M) - \log(n_m)$, transformation of time axis $t \to t'$ which put the position of peaks $t_i, i = 1...(n_M - n_m)$ into a uniform sequence can be written as follows:

$$t'_i = t_{max} - (t_{max} - t_{min})\frac{1 - e^{-\omega i}}{1 - e^{-\omega(n_M - n_m)}}, t < t_c;$$

$$t'_i = t_{min} + (t_{max} - t_{min})\frac{1 - e^{-\omega i}}{1 - e^{-\omega(n_M - n_m)}}, t > t_c. \tag{1}$$

$$\tag{2}$$

This means, near the critical time the time go faster, the "true" time periods are wider than it was measured, and in another side of obervation period it should instead be shorter, ... to keep an overall match to a given time scale.

A

path length — sum of hypotenuses

sum of fitting lines

segment size

10 100   10 000

10   1000
segment size

B

path length

2   20   1000   2   200
segment size

2   20   1000   2   200
segment size

C

periods to c.p.: +2   +10   +100

periods within interval

5

50

from c.p.:   -2   -10   -100

delta correlation: 0.005   -0.005

A; 1; < 10000.

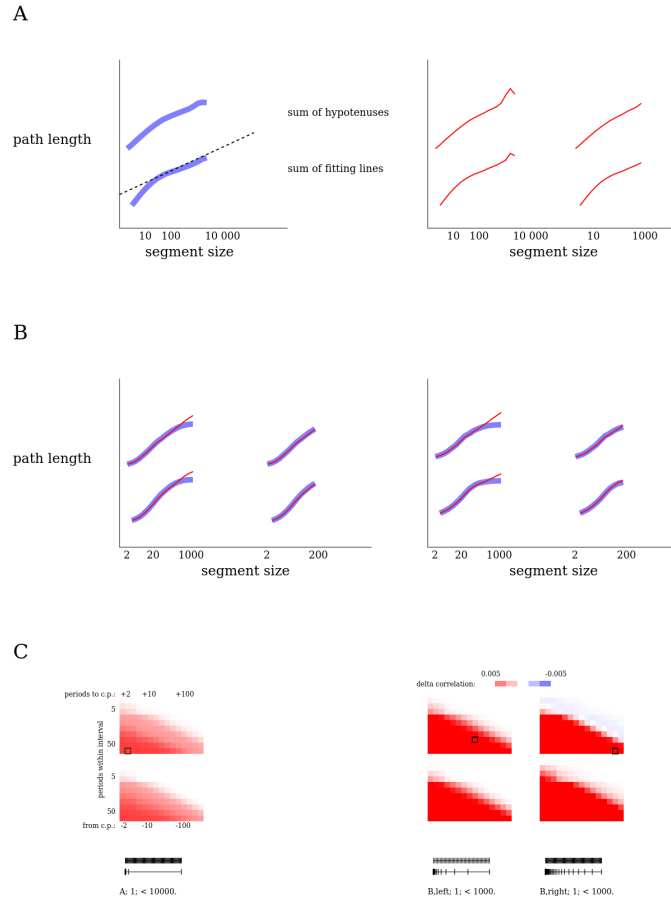B,left; 1; < 1000.   B,right; 1; < 1000.

Figure 2 *Illustrations of attempts to guess a presence of the log-periodic dependency (A) Uniform distribution - chart in fig. 1A (B) Periodic bursts - chart in fig 1B, two parts, 2000 to 2009 and ..., in separate. (C) ...*
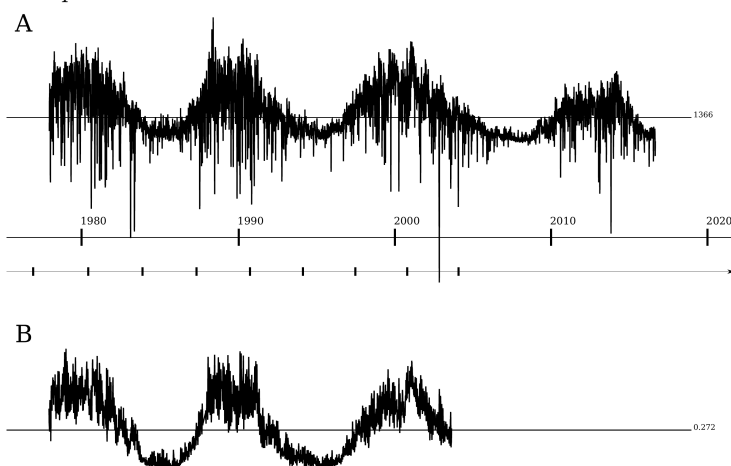
Input measurements

A

B

Figure 3 *(A) Total solar irradiation, November 1978 - September 2017; (B) MgII irradiation, November 1978 - November 2004.*
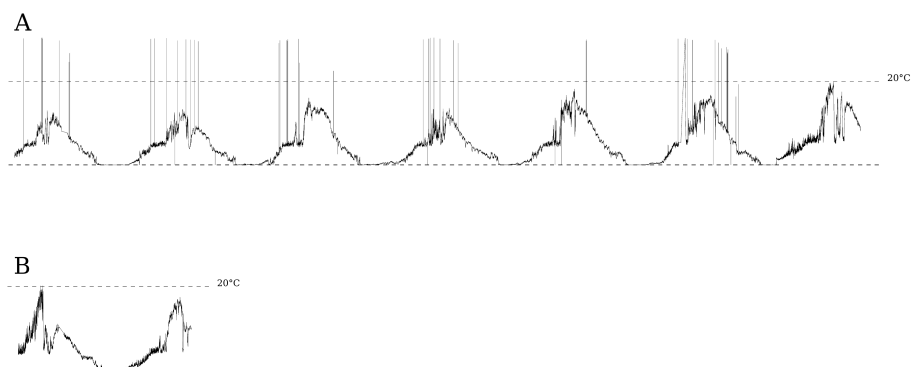
A

B

Figure 4 *Temperature of water in Baikal, (A) - series from May 2010 to October 2016, (B) - series from May 2017 to September 2018.*
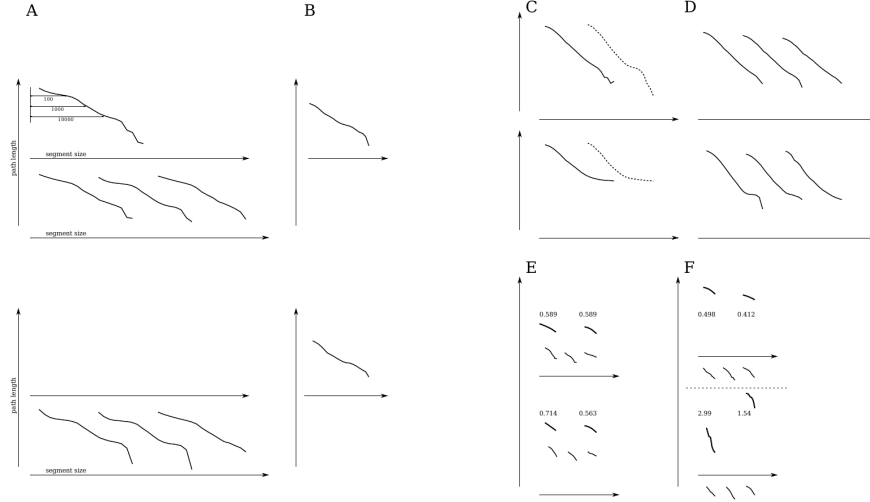
Results

Figure 5 *Log-log dependencies, for the two types of method. A,B: temperature in Baikal, A - 2010-2016, B - 2017-2018 period, C,D: solar activity, 1978-2017, E,F - fragments of auxiliary records on solar irradiation*

In A,D, three separate lines are the distributions for beginning, middle and ending parts of a period. Dashed lines in C, for a comparison - path lengths are estimated by the modified approach, suitable to fitting of log-perodicity. In E,F, - time series are of 15.06.2002 as in fig.2, and of 01.04.2018 as in fig1B, at average and in a few randomly choosed parts. Appropriate fragments from the long-time series, shown in fig 4 and here in C,D, are added for a comparison; numerical labels are estimated least-square slopes of regression lines.

That is, the measure of fractal dimension is consistent for mulitiple data sources. And, the interval $s < 10$ is most sensitive (in fig 5A) to a change of time period.

Total Solar Irradiation, 1978-2018

contraction to future

periods to c.p.: +2   +10   +100

correlation: higher (+)   lower (-)

5

periods within interval

50

5

50

from c.p.: -2   -10   -100

expansion from past

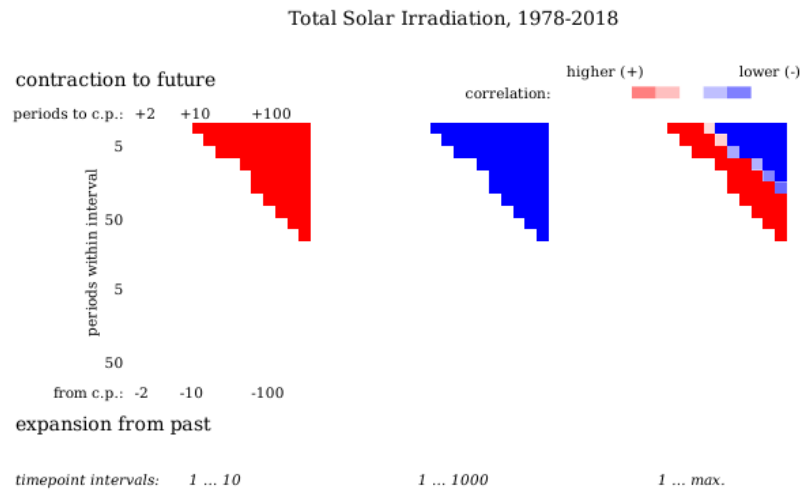timepoint intervals: 1 ... 10   1 ... 1000   1 ... max.

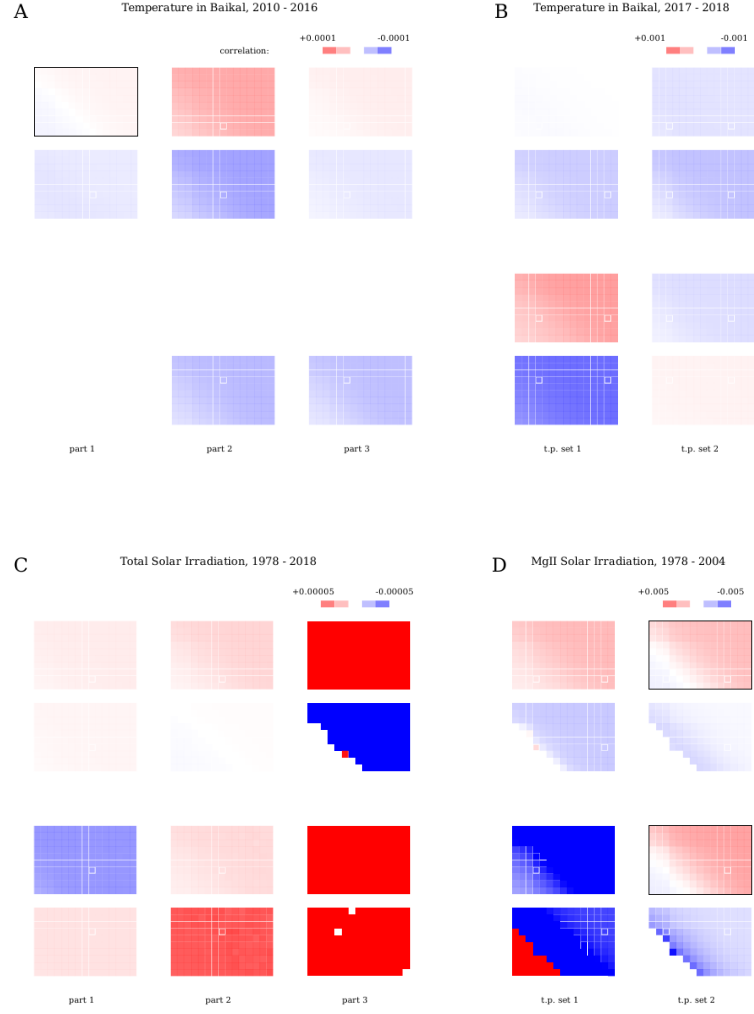Figure 6 *Fitting of log-periodicity. Explanation.*

Figure 7 *Fitting of log-periodicity in separated time periods. Parameters are systematicale listed in table 2.*

That is, for data in fig 7A, a trend to contraction to up-going crisis is observed in the first row. The same trend can be seen in fig 7D for solar activity.

9

Conclusions

The crisis on Baikal which began at around 2014 was possible to detect by slightly unusual variations of water temperature in two to four years before (fig 8 A).

If a covid-19 is not an ordinary virus pandemy, to what extent is this extraaordiunarity expanded? The exclusive search gave similarity of "projection" to a model of log-periodic acceleration between variations of temperature in Baikal before crisis, and variations of intensity of solar irradiation in past 30 years (fig. 8 B), this can point out to expectations of universe-scale crisis in a near future.
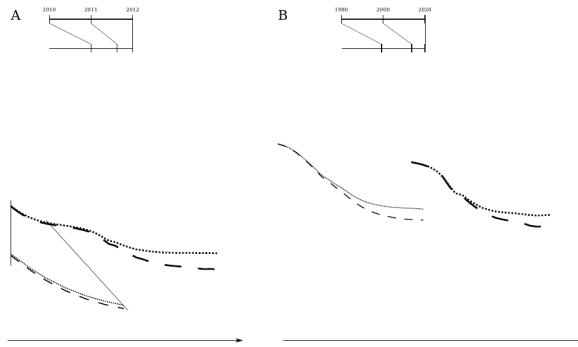

Figure 8 *Concluding drawing.*

References

1. Higuchi, *Phys.Rev*, 19..

2. Peng C.-K., et al., Mosaic organization of DNA nucleotides, *Phys.Rev.*, 1994.

3. Nottale, L., Scale relativity and fractal space-time: theory and applications, *arxiv.org*, 2008

4. Feranchuk, S., Belkova, N., et al. *Limnology and Freshwater Biology*, 2018,

Appendix A

Table 1 *Supplement to figure 2 - results of fitting of log-periodicity in log-log distributions*

	usc_18		acrim3-1		acrim3-2	
	method 1	method 2				
plain:						
dimension	0.577973	0.579382	0.624222	0.667683	0.4569474	0.477499
correlation	0.983925	0.969044	0.97411	0.958568	0.94348	0.922355
fit in full:						
direction	accel.	accel.	accel.	accel.	deccel.	deccel.
critical time	+28	+94	+63	+13	-19	-63
dimension	0.697891	0.621803	0.785739	0.865593	0.706591	0.687815
correlation	0.991618	0.978947	0.998469	0.996726	0.99833	0.990325
fit in part:						
direction	accel.	accel.	accel.	accel.	deccel.	accel.
critical time	+3	+94	+474	+13	-314	+711
dimension	0.66833	0.65472	0.7813	0.908882	0.710503	0.703412
correlation	0.993703	0.972722	0.996467	0.995446	0.9983497	0.995904

Table 2

	method 1		*method 2*	
	dimension	correlation	dimension	correlation
Solar activity,				
total, 1-10 t.p.				
period 1, at a whole	0.611359	-0.98176	-0.98176	-0.992606
period 1, split to 10 parts	0.620717 ± 0.0686381		0.633088 ± 0.117143	
period 2, at a whole	0.582742	-0.980571	0.56841	-0.987462
period 2, split to 10 parts	0.577533 ± 0.0646417		0.57153 ± 0.0621609	
period 3, at a whole	0.529598	-0.98341	0.940431	-0.961894
period 3, split to 10 parts	0.543816 ± 0.117594		0.674605 ± 0.273296	
MnII intensity,				
1...10 t.p., at a whole	0.349931	-0.975307	0.439804	-0.942881
1...10 t.p, split to 10 parts	0.345247 ± 0.102797		0.35548 ± 0.195736	
1...max t.p., at a whole	0.531589	-0.960948	0.560595	-0.930574
1...max t.p, split to 10 parts	0.679449 ± 0.0622246		0.774685 ± 0.109925	
Temperature in Baikal				
long series; 1...10 t.p.				
period 1, at a whole	0.570939	-0.992162	0.812175	-0.995154
period 1, split to 10 parts	0.613501 ± 0.126926		0.868055 ± 0.177196	
period 2, at a whole	0.532256	-0.991045	0.739015	-0.994156
period 2, split to 10 parts	0.633994 ± 0.217527		0.876311 ± 0.29755	
period 3, at a whole	0.303322	-0.99865	0.385959	-0.995293
period 3, split to 10 parts	0.364181 ± 0.227035		0.467551 ± 0.320929	
short series				
1...80 t.p., at a whole	0.606348	-0.995202	0.662082	-0.988346
1...80 t.p., split to 10 parts	0.564113 ± 0.164664		0.628443 ± 0.215225	
40...80 t.p., at a whole	0.508056	-0.981986	0.507846	-0.99867
40...80 t.p, split to 10 parts	0.425593 ± 0.28323		0.444415 ± 0.282211	

Appendix B

```
 cat usc_18.txt | awk -v i=0 -v b1=2458119.5 -v b13=7 '{ if ( i == 100 && substr(
$13, 1, 1 ) != "0" ) { s = s "," 10 * ( $1 - b1 ) "," 500 * (substr($13,1,7)
- b13 ); i = 0; }; i = i+1; } END { print substr( s, 2 ) }' | ./fractal_dimension
-d_xy
```